Research Square

Preprints are preliminary reports that have not undergone peer review.
They should not be considered conclusive, used to inform clinical practice,
or referenced by the media as validated information.

Finite Element Analysis of Stress Distribution in Different Connector Designs of Zygomatic Implant–Supported Prosthetic Rehabilitation for Bilateral Maxillary Defects

Hao Bai
Shanxi Medical University School and Hospital of Stomatology
Wenyan Wu
Ruijin Hospital Affiliated to Shanghai Jiao Tong University School of Medicine
Jiannan Liu
Shanghai Ninth People's Hospital, College of Stomatology, Shanghai Jiao Tong University School of Medicine
Zhen Wang
pmxcl@me.com

Shanghai Ninth People's Hospital, College of Stomatology, Shanghai Jiao Tong University School of Medicine

Research Article

Keywords: Zygomatic Implants, Finite Element Analysis, Zygomatic Implant–Supported Prosthesis, Maxillary Defects

Posted Date: March 13th, 2026

DOI: https://doi.org/10.21203/rs.3.rs-8857722/v1

License: This work is licensed under a Creative Commons Attribution 4.0 International License.
Read Full License

Additional Declarations: No competing interests reported.

Finite Element Analysis of Stress Distribution in Different Connector Designs of Zygomatic Implant–Supported Prosthetic Rehabilitation for Bilateral Maxillary Defects

Running Title: FEA of Connector Designs in Zygomatic Implant Prostheses

Hao Bai [1, #] Wenyan Wu, DDS, MD, PhD [2, #] Jiannan Liu, DDS, MD, PhD [3, *] Zhen Wang, DDS, MD, PhD [3,*]

[1] Shanxi Province Key Laboratory of Oral Diseases Prevention and New Materials, Shanxi Medical University School and Hospital of Stomatology, Taiyuan, PR China.

[2] Department of Stomatology, Ruijin Hospital Affiliated to Shanghai Jiao Tong University School of Medicine, Shanghai, PR China.

[3] Department of Oral and Maxillofacial-Head and Neck Oncology, Shanghai Ninth People's Hospital, College of Stomatology, Shanghai Jiao Tong University School of Medicine; National Clinical Research Center for Oral Diseases; Shanghai Key Laboratory of Stomatology & Shanghai Research Institute of Stomatology, Shanghai, PR China.

[#]Hao Bai and Wenyan Wu contributed equally to this work.

*Correspondence

Dr. Jiannan Liu

Department of Oral and Maxillofacial-Head and Neck Oncology, Shanghai Ninth People's Hospital, College of Stomatology, Shanghai Jiao Tong University School of Medicine; National Clinical Research Center for Oral Diseases; Shanghai Key Laboratory of Stomatology & Shanghai Research Institute of Stomatology,

Shanghai,

P. R. China.

Email: Laurence_ljn@163.com

Dr. Zhen Wang,

Department of Oral and Maxillofacial-Head and Neck Oncology, Shanghai Ninth People's Hospital, College of Stomatology, Shanghai Jiao Tong University School of Medicine; National Clinical Research Center for Oral Diseases; Shanghai Key Laboratory of Stomatology & Shanghai Research Institute of Stomatology,

Shanghai,

P. R. China.

Email: pmxcl@me.com

Acknowledgments

This work was sponsored by the Interdisciplinary Program of Shanghai Jiao Tong University (project No. YG2022QN054)

Conflicts Of Interest

The authors have no conflicts of interest to declare.

CRediT authorship contribution statement

Hao Bai: Conceptualization, Data curation, Formal analysis, Project administration, Resources, Writing – original draft.

Wenyan Wu: Investigation, Formal analysis, Supervision, Visualization, Project administration, Writing – review & editing.

Jiannan Liu: Methodology, Software, Investigation, Validation, Supervision, Project administration, Writing – review & editing.

Zhen Wang: Conceptualization, Investigation, Validation, Supervision, Funding acquisition, Project administration, Resources, Writing – review & editing.

Abstract

Objectives

This study used finite element analysis to compare the biomechanical behavior of ring, horseshoe, and bilateral independent connectors in zygomatic implant-supported prostheses for bilateral maxillary defects, analyzing stress distribution and load transfer to guide connector design optimization.

Materials and Methods

Five patients with bilateral maxillary defects rehabilitated using zygomatic implant–supported prostheses were included. Postoperative CBCT data were used to reconstruct patient-specific skull bone models and zygomatic implant structures. Three restorative configurations—ring-shaped, horseshoe-shaped, and bilateral independent—were constructed with their respective connector frameworks and prostheses. All models were meshed in 3-matic and analyzed in ANSYS Workbench under vertical, lateral, and combined loading conditions. Maximum von Mises stresses in the bone, implant–connector complex, and prosthesis were calculated and compared across configurations.

Results

Marked differences were observed among the three structures. Vertical and combined

loads generated higher stresses than lateral loads, with stress concentration mainly at the implant–abutment junction and the zygomatic bone interface. The ring-shaped connector showed the most uniform stress distribution and the lowest peak stress, compared with the horseshoe-shaped and bilateral independent designs.

Conclusions

Connector configuration significantly influences the biomechanics of zygomatic implant-supported prosthetic systems. The ring-shaped connector, by forming a bilateral closed mechanical loop, evenly distributes occlusal loads and minimizes local stress concentration, demonstrating superior load dispersion and structural stability. It represents an optimal design strategy for bilateral maxillary defect rehabilitation.

Key Words

Zygomatic Implants, Finite Element Analysis, Zygomatic Implant–Supported Prosthesis, Maxillary Defects.

1 | Introduction

Extensive maxillary defects, particularly bilateral maxillary defects, often result from malignant tumor resection, severe trauma, or infection, leading to profound impairment of mastication, speech, and facial esthetics, thereby substantially compromising patients' quality of life.(Mittal, Sharma, Kalra, & Sharma, 2018) In recent years, zygomatic implants—anchoring directly into the dense cortical bone of the zygoma—have emerged as a reliable, graft-free solution for patients with bilateral maxillary defects in whom conventional implant placement is not feasible without prior

bone reconstruction. This technique has become an important treatment option for patients with extensive maxillary defects.(Hackett, El-Wazani, & Butterworth, 2021) Compared with conventional implants that rely on residual maxillary bone, zygomatic implants reduce the need for complex grafting procedures, shorten treatment time, and provide a predictable solution for patients unsuitable for bone augmentation or those seeking immediate functional recovery.(Bedrossian, Rangert, Stumpel, & Indresano, 2006)

The long-term success of implant-supported restorations depends strongly on their biomechanical environment, in which improper occlusal loading is recognized as one of the major risk factors for implant failure.(Oh, Shiau, & Reynolds, 2020) Previous studies have shown that stress distribution within implants is strongly influenced by the design of the prosthetic superstructure, including connector configuration, material stiffness, and overall structural continuity.(Heboyan, Lo Giudice, Kalman, Zafar, & Tribst, 2022; Jain, Sethuraman, & Shah, 2025; Mirchandani, Zhou, Heboyan, Yodmongkol, & Buranawat, 2021) These parameters not only determine how stress is transmitted and concentrated between the implant and surrounding bone but also directly affect bone remodeling and the long-term success of osseointegration. Accordingly, understanding how different connector configurations behave under functional loading is essential for reducing mechanical complications, and enhancing the long-term reliability of zygomatic implant-supported reconstructions.

In the rehabilitation of bilateral maxillary defects, the absence of anterior bone support often necessitates mechanical linkage between the bilateral zygomatic implants

through a connecting framework. Currently, three main types of connector configurations are commonly used in clinical practice: the ring-shaped connector, the horseshoe-shaped connector, and the bilateral independent bar-retained connector.(Gü mrükçü, Balaban, & Bayramoğlu, 2024; Wang, Wu, Zhang, Liu, & Qu, 2021; Xu, Lv, Zhou, & Wang, 2024) While these designs have demonstrated clinical applicability, their mechanical responses under complex occlusal loading have yet to be comprehensively evaluated. Notably, most existing finite element studies are based on a single patient model or idealized geometries, failing to account for interindividual variations in anatomy, implant angulation, and insertion depth, which limits the clinical applicability and generalizability of their findings(Acar, Ari, & Tosun, 2024; Bakay, Gulsun, & Guler, 2025; Costa, Penteado, & Maior, 2023; Heboyan, Lo, Kalman, Zafar, & Tribst, 2022).

To address these limitations, this study established patient-specific three-dimensional finite element models based on clinical data from multiple patients, accurately reflecting individual anatomical characteristics. By applying different occlusal loading conditions, the biomechanical behaviors of three treatment configurations were compared to determine which design exhibited superior biomechanical performance.

2 | Materials and Methods

This study was conducted using clinical and radiographic data from previously treated patients. Ethical approval was obtained from the Ethics Committee of Shanghai

Ninth People's Hospital, Shanghai Jiao Tong University School of Medicine (Approval No. SH9H-2019-T104-2). The study followed the principles of the Declaration of Helsinki and relevant institutional and national research guidelines. Given its retrospective nature, the requirement for individual informed consent was waived by the committee.

2.1 | Patients and Data Acquisition

Five patients with bilateral maxillary defects resulting from tumor resection and subsequently rehabilitated using zygomatic implant–supported prostheses were included. All patients demonstrated satisfactory functional recovery and successful reintegration into daily activities, as confirmed during postoperative follow-up. The clinical characteristics of these individuals—including sex, age, underlying tumor pathology, and the lengths of the four zygomatic implants placed in each case—are summarized in Table 1.

Postoperative CBCT scans were collected and used to construct patient-specific 3D finite element models that accurately reproduced the actual clinical conditions. Three restorative configurations—ring-shaped, horseshoe-shaped, and bilateral independent connectors—were established as the main comparative variables.

2.2 | Model Construction

CBCT images in DICOM format were imported into Mimics 21.0 (Materialise, Belgium) for 3D reconstruction. After threshold segmentation, the STL files were exported and refined in Geomagic Warp 2021 software (Geomagic, USA) to repair surface defects and smooth local geometry, ensuring model continuity. Based on the

manufacturer's specifications (Brånemark System Zygomatic Implant, Nobel Biocare), zygomatic implant models were constructed in Rhinoceros software (Rhino, Robert McNeel & Associates, USA) and combined with three connector configurations and corresponding prostheses (Figure 1).

All components were assembled in Materialise 3-matic (Materialise, Leuven, Belgium) to ensure spatial alignment with clinical implant positions, angulations, and emergence points. Considering the geometric complexity at the implant–abutment–connector interface, moderate surface smoothing was applied to enhance computational efficiency while preserving mechanical accuracy.

2.3 | Finite Element Analysis

The assembled models were imported into ANSYS Workbench (ANSYS Inc., USA) for finite element analysis. All materials were assumed to be continuous, homogeneous, isotropic, and linearly elastic, with material properties listed in Table 2(Ayllón, Navarro, Vázquez, & Domínguez, 2014; Yemenoglu et al., 2025). Bonded contact was assigned to the implant–bone interface to represent full osseointegration, and the same contact definition was applied between the implant–connector complex and the prosthesis (Chen et al., 2017; Magomedov et al., 2025).

A simulated masseteric load of 300 N was applied bilaterally to the muscle insertion areas on the zygomatic arch and zygomatic process of the maxilla. The force vector was decomposed into components of 12.42 N (x-axis), 53.04 N (y-axis), and 25.14 N (z-axis), reproducing the downward, backward, and inward traction of the masseter muscles during mastication (Ishak, Abdul, Sulaiman, & Abu, 2012).

Additionally, a 300 N vertical load was applied to the palatal cusps of the premolars and molars, and a lateral load of 50 N was applied to each side from the palatal toward the buccal direction to simulate functional occlusion (Varghese & Kurian et al., 2023). All loads were distributed across the corresponding contact surfaces to replicate realistic clinical loading conditions. The superior skull and occipital foramen magnum regions were fully constrained to prevent rigid body displacement (Li et al., 2023; Xu, Lv, Zhou, & Wang, 2024). The assembled finite element model is shown in Figure 2.

For each patient, the three connector configurations were analyzed under vertical, lateral, and combined loading conditions. The resulting maximum von Mises equivalent stress (MPa) was calculated for the skull bone, implant–connector complex, and prosthesis. Stress distribution patterns, peak stress values, and concentration regions were visualized using color-coded maps to evaluate the biomechanical performance of each design.

2.4 | Statistical Analysis

To minimize interindividual variability, the stress data from all five patient-specific models were averaged for each connector type and loading condition. Descriptive statistical methods were applied to summarize the results and identify representative biomechanical trends for comparative evaluation among the three connection designs.

3 | Results

Finite element analysis was successfully performed for all five patient-specific models using three connector configurations—ring-shaped, horseshoe-shaped, and bilateral independent—under vertical, lateral, and combined loading conditions.

The analysis yielded the maximum von Mises stress values for the skull bone, implant–connector complex, and prosthesis, which were averaged across all patients to minimize individual anatomical variability and ensure representative biomechanical comparison among the three designs.

3.1 | Vertical Loading

Under a 300 N vertical load, all three connector configurations exhibited comparable overall stress distribution patterns.

As shown in Figure 3, the mean maximum von Mises stress in the skull bone ranged from 44 to 61 MPa, with the horseshoe-shaped connector exhibiting slightly higher values than the other two designs. The implant–connector complex demonstrated the highest stress levels, approximately 190 to 310 MPa, indicating that vertical loading was primarily absorbed within the implant system. The prosthesis exhibited comparatively low stress values, approximately 19 to 26 MPa. Representative stress distribution maps for a typical patient are presented in Figure 4.

3.2 | Lateral Loading

Under bilateral 50 N lateral loading, all three connector configurations showed markedly lower stress levels compared with the vertical loading condition, as illustrated in Figure 5 and Figure 6.

The maxillary bone exhibited von Mises stresses ranging from 6.8 to 7.3 MPa,

while the implant–connector complex showed values around 20–23 MPa, and the prosthesis approximately 7 MPa. Differences among the three connection types were minor, with the horseshoe-shaped connector presenting slightly higher local stresses around the implant region.

3.3 | Combined Loading

When vertical (300 N) and lateral (50 N) loads were applied simultaneously, the overall stress magnitudes further increased, as illustrated in Figure 7 and Figure 8.

The maxillary bone exhibited von Mises stresses ranging from 44 to 60 MPa, comparable to those observed under vertical loading. The implant–connector complex showed a pronounced stress rise (approximately 190–310 MPa), with the bilateral independent connector displaying the highest concentration. The prosthesis maintained a relatively stable range between 19 and 26 MPa.

3.4 | Stress Localization Pattern

Across all patient-specific models, stress concentration was consistently localized at two critical regions—the implant–abutment junction and the interface where the zygomatic implant penetrated the maxillary bone. The dominant stress site varied slightly among patients: in some models, peak stress was concentrated around the implant–bone interface, whereas in others it was observed at the abutment connection (Supplementary Figure S1-S2).

4 | Discussion

In contrast to many published FEA studies that typically relied on a single

idealized model, this study utilized clinical and radiographic data from multiple patients to construct individualized zygomatic implant finite element models. This approach provided a more realistic representation of clinical variability, capturing patient-specific differences in zygomatic morphology and implant spatial configuration. Despite these interindividual variations, the ring-shaped connector consistently demonstrated superior stress control within the zygomatic implant–supported rehabilitation system, achieving more uniform load transmission and balanced stress dispersion under complex loading conditions.

Overall, stress levels under vertical and combined loading were markedly higher than those observed under lateral loading, consistent with the predominance of vertical occlusal forces in clinical function. Across all models, the highest von Mises stresses were consistently concentrated in two mechanically sensitive regions: the implant–abutment junction and the implant–bone interface along the zygomatic bone. These areas therefore represent potential structural weak points that should be carefully considered during surgical placement and prosthetic design. From a biomechanical standpoint, all three connector configurations exhibited maximum von Mises stress values well below the yield strength of titanium, approximately 900 MPa (Akkoyun & Pergel, 2025). The values were also lower than the tensile (≈150 MPa) and compressive (≈250 MPa) strength limits of cortical bone (Wen et al., 2014). These findings indicate that, under the simulated loading conditions, none of the designs imposed detrimental stress on the zygomatic bone or implant components, and all maintained an adequate margin of biomechanical safety at the bone–implant interface.

Clinically, the identified high-stress zones correspond closely to the sites where mechanical complications are frequently reported in zygomatic implant–supported rehabilitations. Localized stress concentration at the implant–abutment junction leads to fatigue-related loosening or fracture of screws and abutments, resulting in prosthetic instability or functional impairment (Brennand et al., 2023). Similarly, excessive stress at the implant–bone interface accelerates marginal bone resorption and compromises osseointegration, increasing the risk of long-term implant failure (Varghese & Gandhi et al., 2023). These clinical correlations underscore the importance of optimizing connector design to reduce concentrated stress and enhance the long-term stability of zygomatic implant systems.

The ring-shaped connector facilitated more balanced load distribution across the bilateral framework, reducing localized stress peaks and maintaining stable structural behavior under combined loading. These findings support the mechanical superiority of the ring-shaped connector in rehabilitating complex bilateral maxillary defects and provide a biomechanical basis for optimizing zygomatic implant framework design and minimizing load-related complications. Future work could integrate patient-specific 3D printing and computational optimization algorithms to refine the geometry and material characteristics of ring-shaped frameworks, thereby achieving reconstructions that better conform to physiological loading conditions and enhance long-term clinical performance (Davoodi et al., 2022).

It should be noted that several modeling simplifications were necessary to highlight the principal load-transfer mechanisms among the connector designs.

Although bone anisotropy and dynamic masticatory behavior were not fully incorporated, the models effectively captured the key biomechanical differences and yielded clinically meaningful insights. Future studies integrating more complex biological properties and time-dependent loading conditions are needed to further validate and extend these findings.

Conclusion

In conclusion, this finite element analysis systematically compared the biomechanical performance of three connector configurations used in zygomatic implant–supported rehabilitation. The findings demonstrated that the ring-shaped connector consistently provided more favorable stress distribution and structural stability under vertical, lateral, and combined loading conditions, confirming its mechanical advantage in the restoration of complex maxillary defects. These results are consistent with clinical performance and offer important theoretical support for the structural optimization and individualized design of zygomatic implant rehabilitation systems.

Funding

This work was sponsored by the Interdisciplinary Program of Shanghai Jiao Tong University (project No. YG2022QN054)

Tables:

Table 1. Demographic and Clinical Characteristics of the Included Patients

Patient ID	Sex(M/F)/age (years)	Tumor Classification	ZI1 Length (mm)	ZI2 Length (mm)	ZI3 Length (mm)	ZI4 Length (mm)
Patient 1	Female/60	Malignant melanoma	52.5	52.5	52.5	52.5
Patient 2	Female/63	Pleomorphic adenoma	47.5	50	45	37.5
Patient 3	Female/62	Chondrosarcoma	35	37.5	37.5	32.5
Patient 4	Male/59	Oral squamous cell carcinoma	42.5	52.5	45	37.5
Patient 5	Male/56	Oral squamous cell carcinoma	42.5	42.5	35	52.5

Table 2. Material properties used in the finite element analysis

	Young Modulus（MPa）	Poisson Ratio（v）	Component
Ti（TA4）	$1.045*10^5$	0.35	Implant–connector complex
PMMA	2700	0.3	Prosthesis

Cortical Bone	$1.37*10^4$	0.3	Skull bone

Figures:

Figure 1. Three types of connector configurations used in the finite element models.

A: Ring-shaped connector with the corresponding prosthesis.

B: Horseshoe-shaped connector with the corresponding prosthesis.

C: Bilateral independent connectors with the corresponding prosthesis.

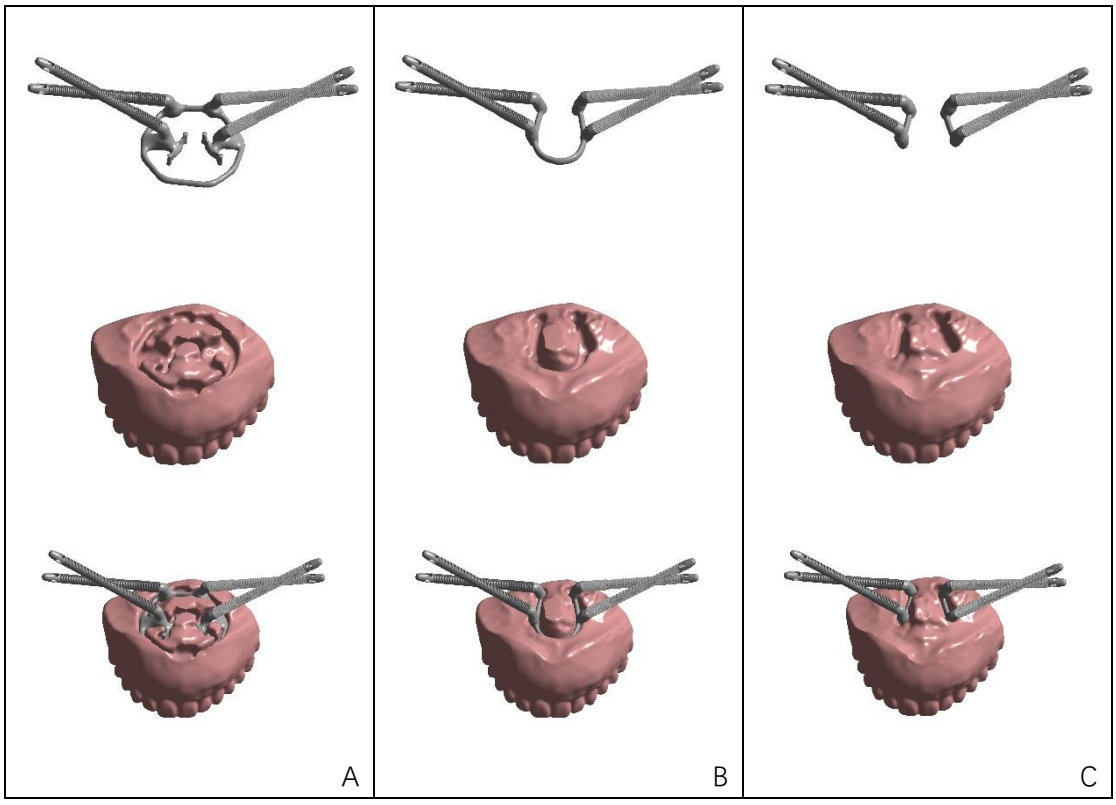


Figure 2. Assembled finite element model in two viewing orientations.

A: Frontal view of the assembled model.

B: Lateral view of the assembled model.

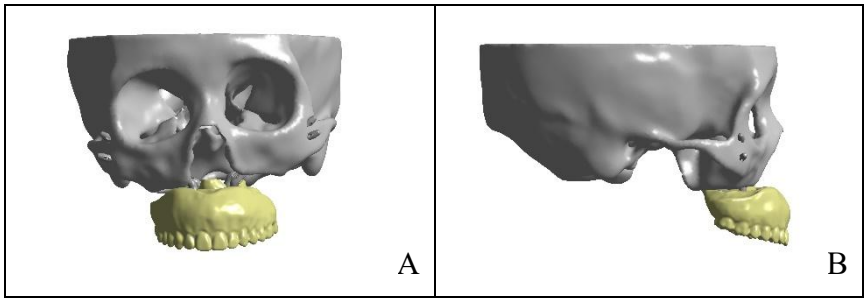


Figure 3. Mean maximum von Mises stress (MPa) of three connector designs under vertical loading. R: Ring-shaped connector; H: Horseshoe-shaped connector; B: Bilateral independent connector.

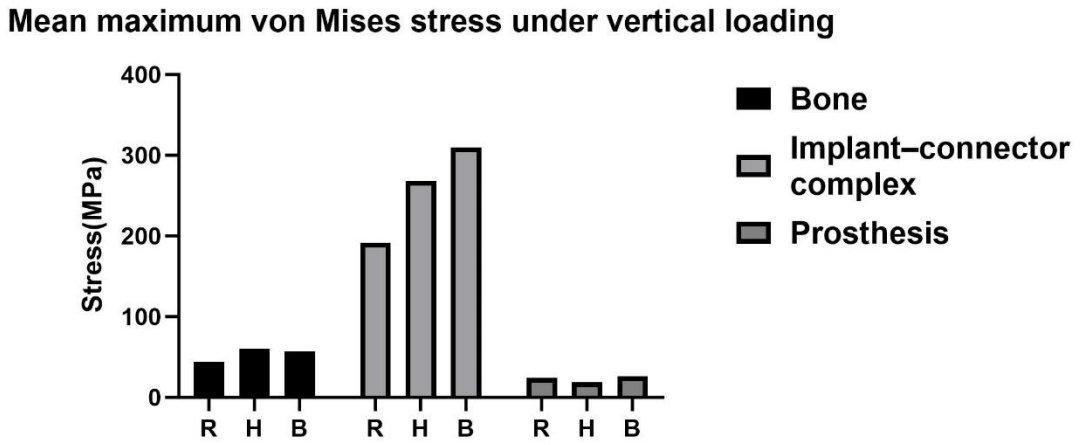


Figure 4. Representative stress distribution maps of the three connector configurations under vertical loading. A: Ring-shaped connector; B: Horseshoe-shaped connector; C: Bilateral independent connector

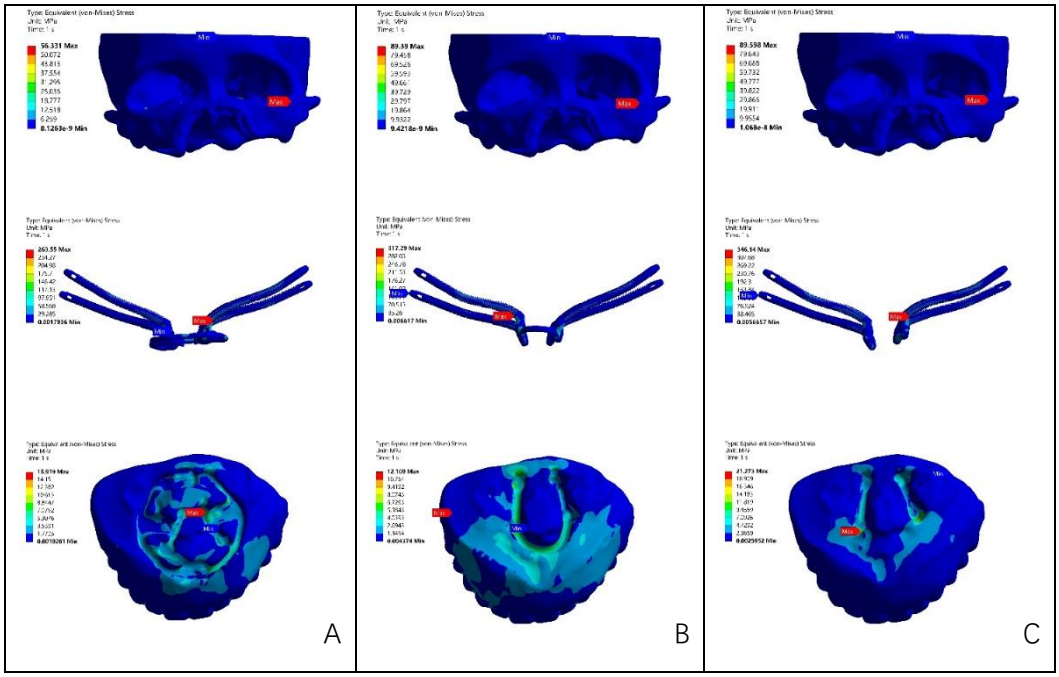


Figure 5. Mean maximum von Mises stress (MPa) of three connector designs under lateral loading. R: Ring-shaped connector; H: Horseshoe-shaped connector; B: Bilateral independent connector.

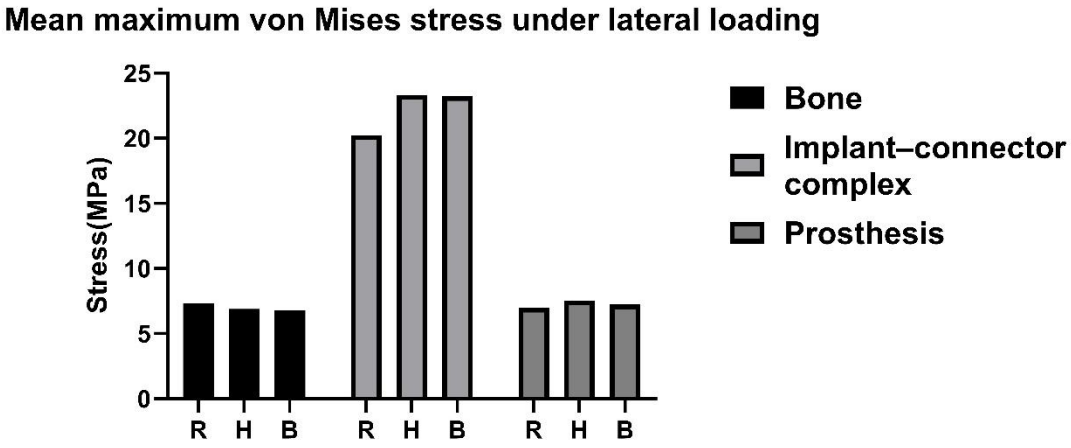


Figure 6. Representative stress distribution maps of the three connector configurations under lateral loading. A: Ring-shaped connector; B: Horseshoe-shaped connector; C: Bilateral independent connector

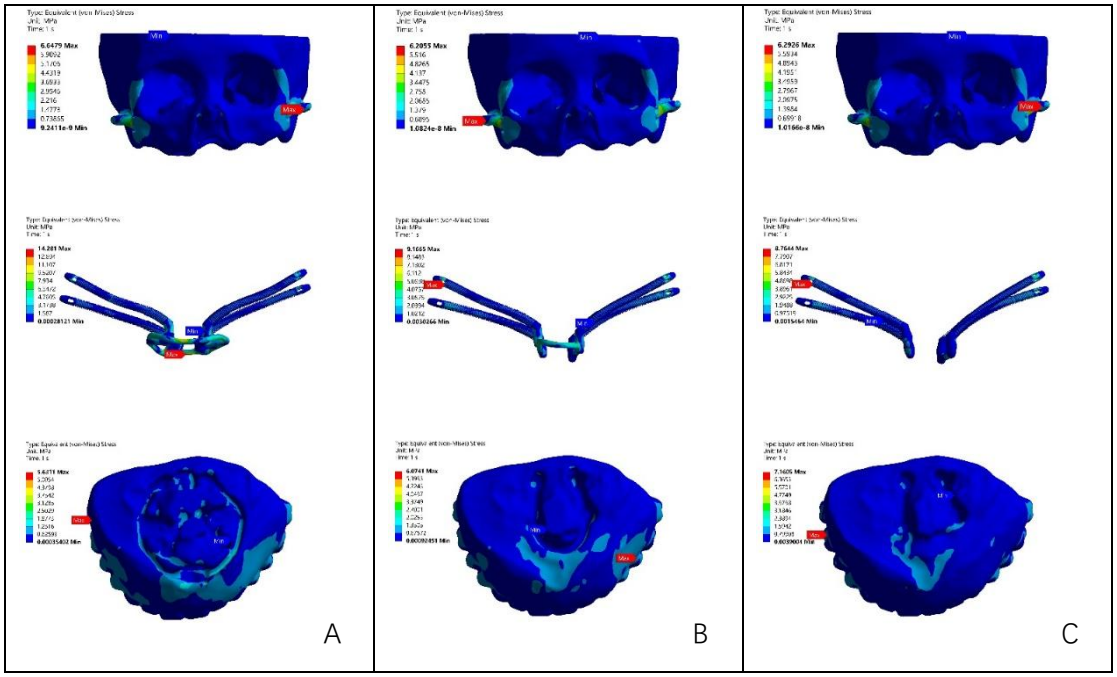


Figure 7. Mean maximum von Mises stress (MPa) of three connector designs under combined loading. R: Ring-shaped connector; H: Horseshoe-shaped connector; B: Bilateral independent connector.

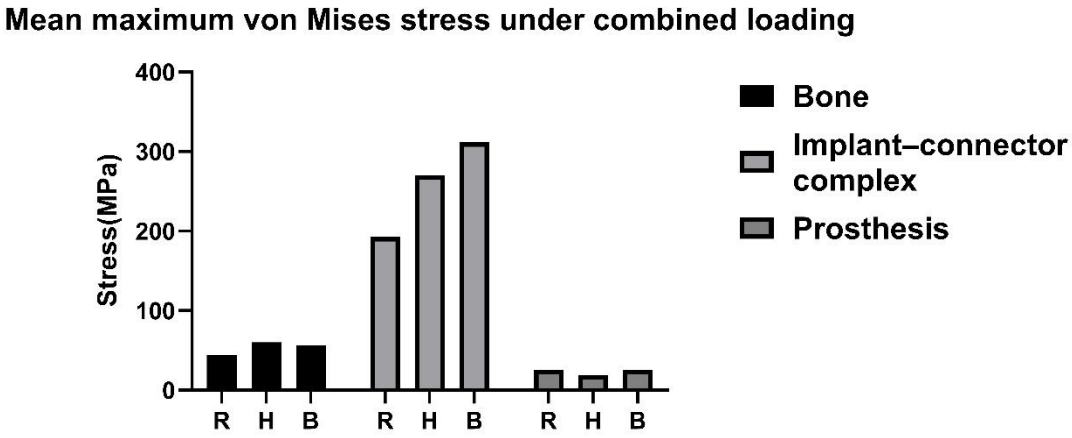
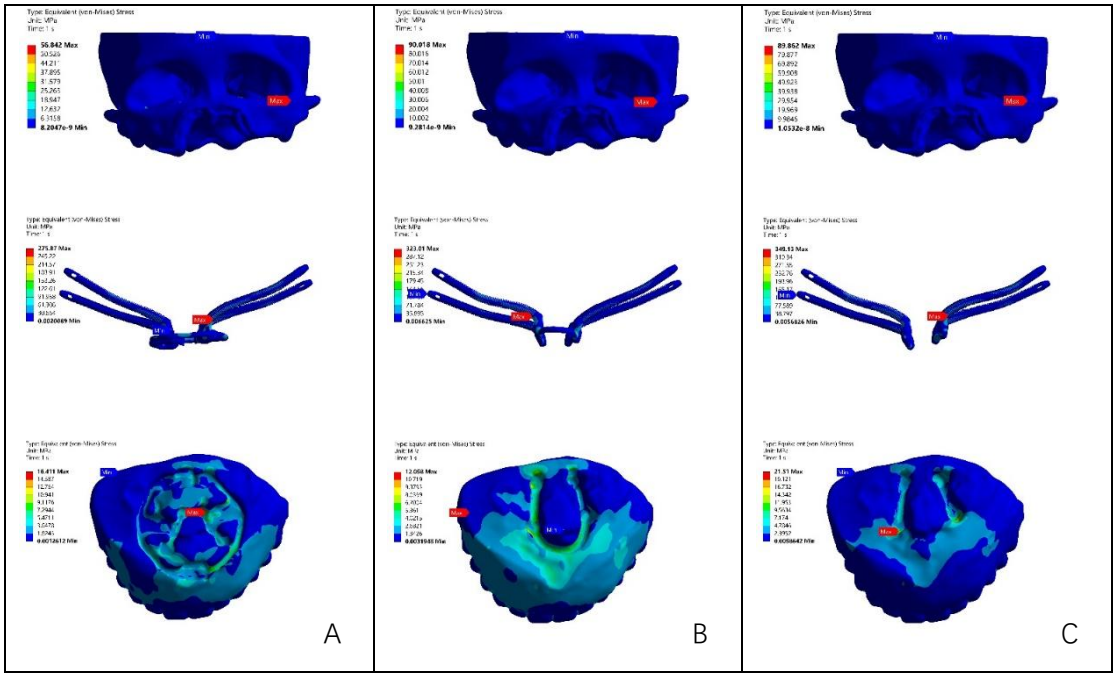


Figure 8. Representative stress distribution maps of the three connector configurations under combined loading. A: Ring-shaped connector; B: Horseshoe-shaped connector; C: Bilateral independent connector



References:

Acar, G., Ari, I., & Tosun, E. (2024). Biomechanical evaluation of implant options for unilateral maxillary defects: a finite element analysis. *BMC Oral Health*, *24*(1), 1338. doi:10.1186/s12903-024-05100-0

Akkoyun, E. F., & Pergel, T. (2025). Finite element analysis of shape and thickness variations in patient-specific implants for t-shaped genioplasty. *Med Oral Patol Oral Cir Bucal*, *30*(4), e528-e535. doi:10.4317/medoral.27065

Ayllón, J. M., Navarro, C., Vázquez, J., & Domínguez, J. (2014). Fatigue life estimation in dental implants. *Engineering Fracture Mechanics*, *123*, 34-43. doi:https://doi.org/10.1016/j.engfracmech.2014.03.011

Bakay, U., Gulsun, B., & Guler, R. (2025). Investigation of the stresses on pterygoid and zygomatic implants used in atrophic maxilla rehabilitation by finite element analysis. *Med Oral Patol Oral Cir Bucal*, *30*(5), e700-e708. doi:10.4317/medoral.27199

Bedrossian, E., Rangert, B., Stumpel, L., & Indresano, T. (2006). Immediate function with the zygomatic implant: a graftless solution for the patient with mild to advanced atrophy of the maxilla. *Int J Oral Maxillofac Implants*, *21*(6), 937-942

Brennand, R. M., Vissink, A., Dudding, T., Pollard, A., Gareb, B., Malevez, C., ... Jung, R. (2023). Long-term treatment outcomes with zygomatic implants: a systematic review and meta-analysis. *Int J Implant Dent*, *9*(1), 21. doi:10.1186/s40729-023-00479-x

Chen, Y., Wang, C., Huang, Y., Feng, T., Zou, H., & Fan, Y. (2017). Biomechanical evaluation of the

natural abutment teeth in combined tooth-implant-supported telescopic prostheses: a three-dimensional finite element analysis. *Comput Methods Biomech Biomed Engin*, *20*(9), 967-979. doi:10.1080/10255842.2017.1319941

Costa, E. F., Penteado, M. M., & Maior, B. S. (2023). Comparative analysis of biomechanical response between zygomatic implant and Facco technique through the three-dimensional finite element method. *J Clin Exp Dent*, *15*(2), e96-e101. doi:10.4317/jced.59885

Davoodi, E., Montazerian, H., Mirhakimi, A. S., Zhianmanesh, M., Ibhadode, O., Shahabad, S. I., ... Toyserkani, E. (2022). Additively manufactured metallic biomaterials. *Bioact Mater*, *15*, 214-249. doi:10.1016/j.bioactmat.2021.12.027

Gümrükçü, Z., Balaban, E., & Bayramoğlu, Z. (2024). Biomechanical evaluation of six zygomatic implants versus four zygomatic implants combined with dental implants in the treatment of different maxillary defects. *BMC Oral Health*, *24*(1), 1230. doi:10.1186/s12903-024-05031-w

Hackett, S., El-Wazani, B., & Butterworth, C. (2021). Zygomatic implant-based rehabilitation for patients with maxillary and mid-facial oncology defects: A review. *Oral Dis*, *27*(1), 27-41. doi:10.1111/odi.13305

Heboyan, A., Lo Giudice, R., Kalman, L., Zafar, M. S., & Tribst, J. P. (2022). Stress Distribution Pattern in Zygomatic Implants Supporting Different Superstructure Materials, *Materials*, Vol. 15).

Heboyan, A., Lo, G. R., Kalman, L., Zafar, M. S., & Tribst, J. (2022). Stress Distribution Pattern in Zygomatic Implants Supporting Different Superstructure Materials. *Materials (Basel)*, *15*(14). doi:10.3390/ma15144953

Ishak, M. I., Abdul, K. M., Sulaiman, E., & Abu, K. N. (2012). Finite element analysis of different surgical approaches in various occlusal loading locations for zygomatic implant placement for the treatment of atrophic maxillae. *Int J Oral Maxillofac Surg*, *41*(9), 1077-1089. doi:10.1016/j.ijom.2012.04.010

Jain, J., Sethuraman, R., & Shah, S. S. (2025). Comparative evaluation of pattern and distribution of stresses in single- and double-implant overdenture using ball-ring, positioner, and magnet-keeper attachment under different loading conditions: A finite element analysis. *J Indian Prosthodont Soc*, *25*(1), 86-94. doi:10.4103/jips.jips_179_24

Li, A., Mu, Z., Zeng, B., Shen, T., Hu, R., Wang, H., & Deng, H. (2023). Evaluation of two treatment concepts of four implants supporting fixed prosthesis in an atrophic maxilla: finite element analysis. *BMC Oral Health*, *23*(1), 983. doi:10.1186/s12903-023-03706-4

Magomedov, M., Kozulin, A., Arutyunov, S., Drobyshev, A., Dibirov, T., Kharazyan, E., ... Panin, S. (2025). Computer Simulation of the Mechanical Behavior of the 'Zygomatic Bones-Implants-Splinting Bar-Removable Overdenture' Dental Structure Under Operational Loads. *Dent J (Basel)*, *13*(9). doi:10.3390/dj13090393

Mirchandani, B., Zhou, T., Heboyan, A., Yodmongkol, S., & Buranawat, B. (2021). Biomechanical Aspects of Various Attachments for Implant Overdentures: A Review. *Polymers (Basel)*, *13*(19). doi:10.3390/polym13193248

Mittal, M., Sharma, R., Kalra, A., & Sharma, P. (2018). Form, Function, and Esthetics in Prosthetically Rehabilitated Maxillary Defects. *J Craniofac Surg*, *29*(1), e8-e12. doi:10.1097/SCS.0000000000003985

Oh, S., Shiau, H. J., & Reynolds, M. A. (2020). Survival of dental implants at sites after implant failure: A systematic review. *J Prosthet Dent*, *123*(1), 54-60. doi:10.1016/j.prosdent.2018.11.007

Varghese, K. G., Gandhi, N., Kurian, N., Daniel, A. Y., Dhawan, K., Joseph, M., & Varghese, M. G.

(2023). Rehabilitation of the severely resorbed maxilla by using quad zygomatic implant-supported prostheses: a systematic review and meta-analysis. *J Prosthet Dent*, *130*(4), 543-552. doi:10.1016/j.prosdent.2021.11.007

Varghese, K. G., Kurian, N., Gandhi, N., Gandhi, S., Daniel, A. Y., Thomas, H. A., ... Wadhwa, S. (2023). Three-dimensional finite element analysis of zygomatic implants for rehabilitation of patients with a severely atrophic maxilla. *J Prosthet Dent*, *129*(4), 591-597. doi:10.1016/j.prosdent.2023.01.012

Wang, Z., Wu, W., Zhang, C., Liu, J., & Qu, X. (2021). "Three-Dimensional Ring" of Zygomatic-Supported Prosthetics Rehabilitation in Bilateral Maxillary Defect. *Int J Oral Maxillofac Implants*, *36*(6), 1235-1246. doi:10.11607/jomi.8799

Wen, H., Guo, W., Liang, R., Xiang, L., Long, G., Wang, T., ... Tian, W. (2014). Finite element analysis of three zygomatic implant techniques for the severely atrophic edentulous maxilla. *J Prosthet Dent*, *111*(3), 203-215. doi:10.1016/j.prosdent.2013.05.004

Xu, S., Lv, J., Zhou, Y., & Wang, K. (2024). Utilizing a Fully Digital Approach for Oral Squamous Cell Carcinoma Treatment and Zygomatic Implant-Based Rehabilitation for Maxillary Defects. *J Oral Implantol*, *50*(6), 595-604. doi:10.1563/aaid-joi-D-24-00115

Xu, S., Lv, J., Zhou, Y., & Wang, K. (2024). Utilizing a Fully Digital Approach for Oral Squamous Cell Carcinoma Treatment and Zygomatic Implant-Based Rehabilitation for Maxillary Defects. *J Oral Implantol*, *50*(6), 595-604. doi:10.1563/aaid-joi-D-24-00115

Yemenoglu, H., Beder, M., Yaylacı, M., Dizdar, A., Alkurt, M., Naralan, M. E., ... Yeşil, Z. (2025). Evaluation of prostheses retained zygomatic and dental implants in large defects in the maxilla due to tumors or major trauma by biomechanical 3- dimensional finite element analysis. *BMC Oral Health*, *25*(1), 99. doi:10.1186/s12903-025-05468-7